Novel image similarity measurement in Automated Optical Inspection

TIBOR TAKÁCS, LÁSZLÓ VAJTA

Budapest University of Technology and Economics,
Department of Control Engineering and Information Technology
{takacs, vajta}@iit.bme.hu

Keywords: image processing, automated optical inspection (AOI), image similarity measurement

Image similarity measurement is one of the most important topics in industrial image processing systems. In automated optical inspection (AOI) in electronic device manufacturing, the widely used methods are built mainly on separated analysis of gray-scale images, and do not apply the high similarity between captured pictures. This paper presents a new methodology to measure the relative similarity of AOI images. Our method utilizes and satisfies the special conditions and requirements of AOI systems. The need for human intervention (parameter adjustment, calibration) is almost totally eliminated. As our experiments show, our novel techniques classify more than 98% of images in the perfect classes which makes the techniques built on this similarity measurement method entirely useful in industrial applications already at this stage of our research.

1. Introduction

Today's electronic device manufacturing factories are unimaginable without modern automated optical inspection (AOI) systems. Humans are expensive and too slow to keep up with the frenetic beat rates of today's assembly lines. Their eyes are not good enough to match the output of ultra-fine manufacturing processes, and we have difficulty keeping focused on very repetitive tasks [14].

Nowadays, the most widespread optical inspection systems in electronic device manufacturing are based on analysis of high-resolution gray-scale camera pictures created by monocular matrix camera. (In this article, we focus mainly on system built up on this principle, especially on post-soldering inspection systems.) The images created by AOI devices have a very special feature which is useful in accurate and reliable quality measurement systems. Namely, the pictures about the same component type are either very similar to, or very dissimilar from each other. Generally, the components with good quality have very similar appearances; however the bad images differ in a high degree *(Fig. 1)*.

This article is about the similarity of AOI images. First, we illustrate the possibilities and difficulties of similarity measurement in optical inspection. Next, we explain our novel similarity measurement method based on image processing, statistical, outlier detection and classification techniques. Finally, we show two important examples in AOI systems (image database filtering, decision support system for human operators) where our algorithm provides an excellent solution.

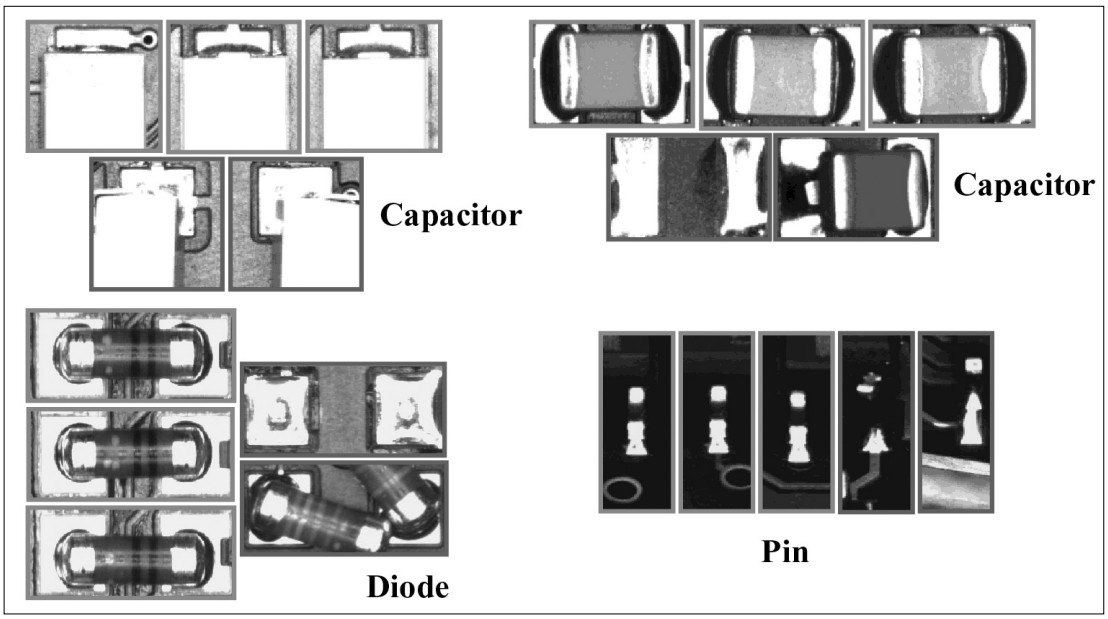

Figure 1. Similarity of AOI images

2. Image similarity measurement in AOI systems

2.1 Process model of AOI system

First of all, we briefly present a generalized ideal model of automated optical inspection systems of post-soldering printed circuit board (PCB) inspection *(Fig. 2)*. By means of this simplified model we explain the environment where our techniques and algorithms can be placed. We present also several keywords which constitute the basic terminology of this article (marked as *italic*).

After a manufacturing step, the PCB is put in the AOI device specified to inspect the errors of previous processes (1). The AOI device loads the parameter values according to the type of the actual PCB (2) and executes the optical inspection procedure *(AOI algorithm, AOI macro)*. (3): the AOI device creates several images, performs image processing algorithms and classifies the components as *"good"* or *"bad"*. The images classified as good are stored in the "good" part of the image database (4). If the PCB contains some errors, it is sent to the repair station with *error information* like error codes, locations and *error images* containing components classified as bad (5). The human operator at the repair station *re-inspects* the received errors. If an error is a *"real error"* (namely the AOI device is right), the PCB will be removed from the manufacturing line (sometimes the human operator can repair the error) and the image containing the bad component is stored in the "error" part of the image base (6).

If the AOI machine failed *(false alarm* or *false-call)*, the image is sent to the "false-call" group in the image database (7). It is also possible that a bad component is not recognized by the AOI devices and it will be identified only at a later manufacturing process or at usage *("slippage")*. The slipped images are also stored in the "error" part of image base later (8).

If the AOI system does not work with appropriate quality (i.e. too many false calls occur, or a slippage is identified), an AOI process engineer optimizes the AOI inspection algorithms (9): he or she tunes the macro's parameters or changes the working process of the algorithm. To verify the optimization's result, he runs the adjusted macro on the old images stored in the image database. If the new algorithm has better inspection quality than the old one, the old will be replaced with the new.

2.2 Background

As mentioned in the Introduction, the images containing good components are very similar to each other, but the real error pictures differ from them (and also from each other) to a high degree. This occurrence motivated us to apply image similarity measurement as classification method. Our algorithm compares the image under inspection with a special image database – which contains good and bad reference images –, and the proposed class is calculated by means of this similarity information.

At this point, the following important question arises: when is an image "enough similar" to a set of good images? Similarity is only a qualitative mark, but for classification in AOI system it is necessary to use quantitative metrics. To determine an exact classification threshold, which is valid for all types of components, is a quite impossible task.

The basis of our technique is that we consider the similarity as a **relative**, but quantitative measurement value. The algorithm calculates a *similarity degree* for all images, also for references and also for actual inspection image. The classification decision can be executed depending on the actual situation (actual similarity degrees of reference images). This principle precludes the mentioned definability question of similarity.

In the following, we present first an overview of the related work. Next we introduce the requirements about a similarity measurement system in field of AOI. Finally, our novel method will be explained how can the similarity degrees of images in an image-database calculated.

Figure 2. Generalized ideal model of AOI systems

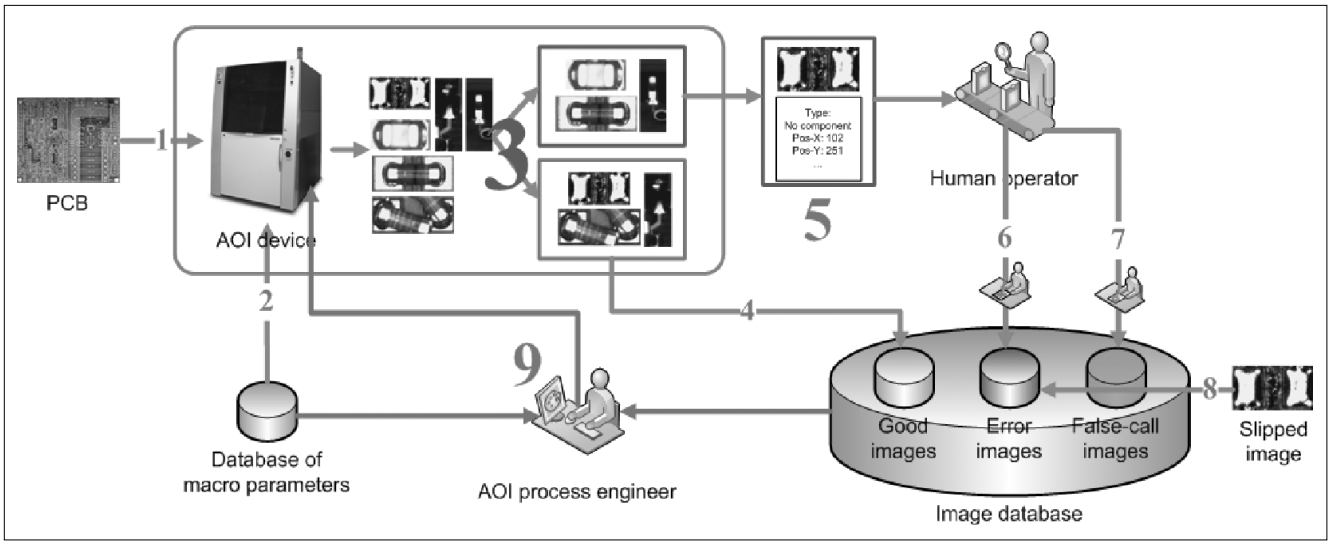

2.3 Related works

In automated optical inspection systems, the image similarity measurement is used to find the images containing faulty components. In the literature and industry, there are two main directions in optical quality measurement.

In the first group, where the most widespread methods are located, the captured images are separately analysed by means of image processing and classification algorithms using several predetermined parameters. They process only the actual images, and they do not take into account information about earlier results.

Wang et al. [22] proposed a new approach using accelerated species based particle swarm optimization for multi-template matching. The method completed the general PSO algorithm to allow the particles to search for multiple optima (either local or global) simultaneously to overcome the deficiency of the original PSO in multimodal optimization problems.

The paper written by Mar et al. [17] presented a computer vision system for automatic detection, localisation and segmentation of solder joints on PCBs under different illumination conditions. After an illumination normalization approach, the PCB image is transformed from an RGB colour space to a YIQ colour space for the effective detection of solder joints from the background. Finally, by thresholding and region filling, the solder joint are segmented and classified.

An interesting solution was proposed by Kong and Wang in 2007 [12]. Their paper deals with the reconstruction of the solder joint's surface in PCB based on shape from shading technology which is an important non-contact measurement method.

The second frequent way in optical inspection of PCBs is the usage of special computational models like artificial neural networks. Acciani et al. in 2006 [1,2] developed a solder joint classification method which uses multiple neural networks. Five different levels of solder quality in respect to the amount of solder paste have been defined. Two feature vectors extracted from the images' region of interest feed the neural network system for the classification.

A complete system to detect mounting defects in the circuits in presented in [5]. The authors processed the AOI images using wavelet transform and neural networks, for low computational cost and acceptable precision.

An artificial neural network (ANN) was used by Ong et al and presented in [18]. They combined orthogonal and oblique gray-level images at pixel level which were then directly input into an ANN for processing, eliminating the need to determine heuristic features. Learning vector quantization architecture was used as the classifier.

These approaches can solve several important problems in field of automated optical inspection, but they have also limitations. Namely, there are several fields of quality inspection in electronic manufacturing where special requirements need to be considered and the current approaches cannot satisfy them.

Our novel similarity measurement technique was developed based on these requirements. In next section, we will present four general conditions which are very important in case of optical inspection algorithm. In Section 3 (3.1, 3.2), we will propose two new approaches built on novel similarity metric where we will show the details of current approaches' limitations and present what the proposed method adds to the state of the art.

2.4 Special requirements

Our main goal is to estimate the appropriate class of an inspection image only by means of a reference image database using image similarity measurement. To produce a well usable classification system, our method needs to satisfy the following requirements:

• **Flexibility**. The general AOI inspection algorithms are rigid measurement methods. After adjusting their parameters, they execute the same steps with same conditions, and they do not react to the manufacturing changes directly and immediately. This is one of reasons of the relative high false call rate. Because our method aims at reducing this problem, it needs to adapt itself to the actual conditions and environment continually and automatically.

• **No parameters**. Our method contains image processing, outlier detection, clustering and statistical algorithms which have several parameters. Our purpose is that the values of these parameters would be calculated by the algorithm during runtime and not by human experts during implementation time. This is also a precondition of flexibility described in previous point.

• **Transparency from image type**. An AOI device inspects several different components creating very different images. We aimed at developing an algorithm which can work on several types of images equally well.

• **No a-priori information about AOI inspection algorithm**. An AOI macro inspects specified region of images and executes special transformations. Our decision support algorithm does not consider this a-priori information to avoid the dependency on the settings of the AOI macro.

2.5 Calculation of similarity degree

The basic idea behind our similarity degree calculation in AOI systems is quite simple. The calculation time of similarity degree is very critical because of high productivity of the modern manufacturing lines. Therefore to compare all error images with all corresponding images is an impossible task in inspection process. This urged us to develop a novel method which can estimate the similarity degree without numerous compare calculations.

To solve this problem, the algorithm creates first a **golden template image** which represents a general case of ideal (good) images. The similarity degree is inherited from the difference between the image and this golden template.

Behind this simple theory, a complicated algorithm lies with the following steps:

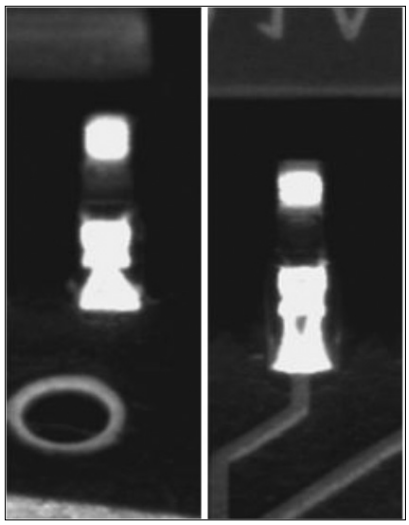

Figure 3. Differences in position of images

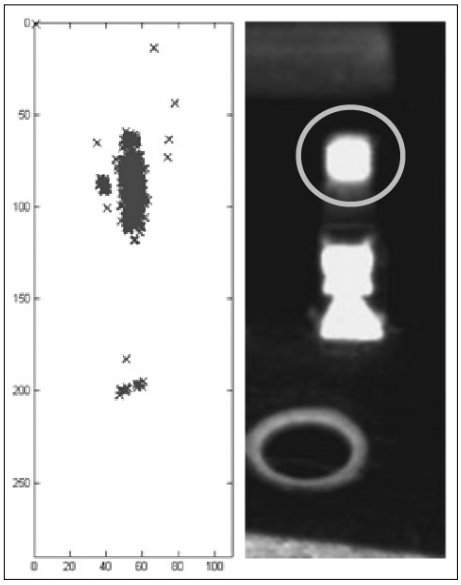

Figure 4. The positions of the reference point in SOIC image base

1. Iterative translation compensation (pre-processing)
2. Calculation of golden template
3. Split into sub-images
4. Calculation of difference profile
5. Estimation of similarity degree

In the following the details of the algorithm will be presented. The results of the processing steps will be illustrated by means of image database about SOIC (small-outline integrated circuit) pins. The dimension of images in image-space is 242x104 pixels, which shows a pin with size 1x0.5 mm.

2.5.1 Iterative translation compensation (pre-processing)

The images showing good components contain very similar features, but unfortunately the location of the important objects can be varied to some degree (see *Fig. 3)*. The reduction of position disparity makes the classification methods faster, easier and more accurate, because similarity measurement can suggest that similar image-features have similar positions. Therefore, as the first step, the position disparities of the actual error image will be compensated.

First, the compensation algorithm looks for the *reference points* of the image. This reference point is a special feature point on the image: centre of mass of the whole image; centre of mass of a specified feature etc. [6]. The choice, which feature point is the best to use, depends on the (component) type of the actual image. (A future research could be to determine a general reference point.) *Fig. 4* illustrates an example of the calculated reference points. In this case, the centre of mass of the white object in the upper part of the image (in green circle) represents the reference point. Therefore the different appearance of wires does not influence the result.

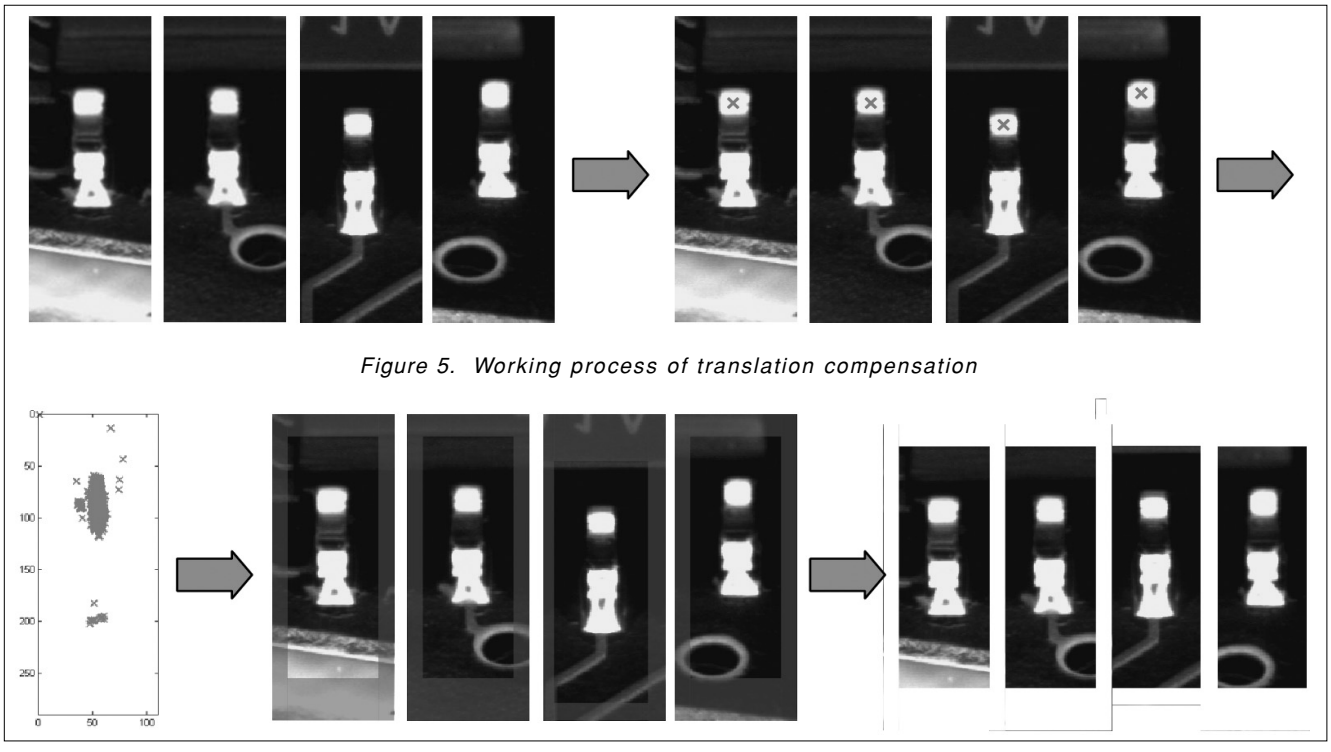

Figure 5. Working process of translation compensation

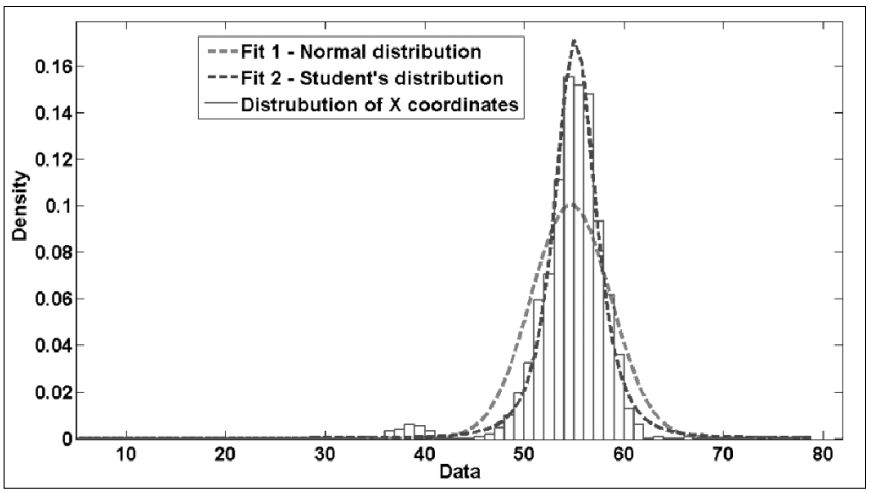

Figure 6. Distribution of X coordinates

In the ideal case, the reference points have the same position on each image, but in a real situation their locations vary to some degree. The goal is to remove these disparities to get the reference points overlapped, resulting that the features on the images will cover each other as well.

Next, the algorithm calculates the expected value of reference points and cuts the sides of each image to move the image's references over the position of the expected value *(Fig. 5)*. This results that the reference points of all images have the same location. The size of cutting depends on the distance between the actual reference and the expected value of all points therefore the bigger this distance the smaller the resulted picture size becomes. Because the images need to have the same size after translation compensation, only one outlier reference point, which is very far from the expected value, produces very small result images losing the most relevant information. Therefore the maximal cutting sizes in both directions were limited to the average distance from the expected value.

The determined bound was a good choice to avoid too small result images while several images' positions were compensated. *Fig. 6* visualizes the distribution of reference points' coordinates. It is interesting to note that the coordinates are not normally distributed. Our experiments show that distributions with best fits are the scaled and translated Student's t-distribution [11] or logistic distribution [3].

The previous steps (determination of reference points, calculating the expected value, cutting image sides to reduce the disparity) can be repeated until the disparities of the reference points fall below a specified limit. Our research showed that after 4 iterations the position improvement of position optimization stopped.

The graphs on *Fig. 7* illustrate the efficiency of this method. They show the standard deviation of pixel values before and after compensation. It is easy to see that after translation compensation the variance of pixels decreased in high degree (most at edges of objects) because the images become more similar to each other.

After translation compensation, the differences between features' positions of different images are roughly eliminated. Small differences in size and location are certainly possible, but large variations are only accepted in case of real error images. This characteristic of compensated image base is used to determine the images' similarity degree.

2.5.2 Calculation of golden template

Next the golden template is calculated which is an "ideal" good image. By its calculation, only the good (and false-call) images are taken into account from the reference image database, because the similarity degree means how the actual image is similar to the good images.

The images can be considered as the samples of a random variable matrix:

$$I = \left(\xi_{ij}\right), \forall \xi_{ij} : \Omega \to \mathbb{R} \tag{1}$$

where *i* and *j* are pixel indices, ξ_{ij} is the random variable, Ω is the space of possible gray-scale values, and $\mathbb{R}$ is the real numbers representing the gray-scale values (typically integer numbers between 0 and 255). The distributions of these variables show the probabilities of the pixels' gray scale values.

The comparison algorithm (as we will introduce soon) is executed on pixel level, therefore it is a reasonable choice to use a matrix created from the expected values of the random variable matrix as golden template [7]:

Figure 7. The effect of iterative translation compensation algorithm (the standard deviation of pixels decreased substantially)

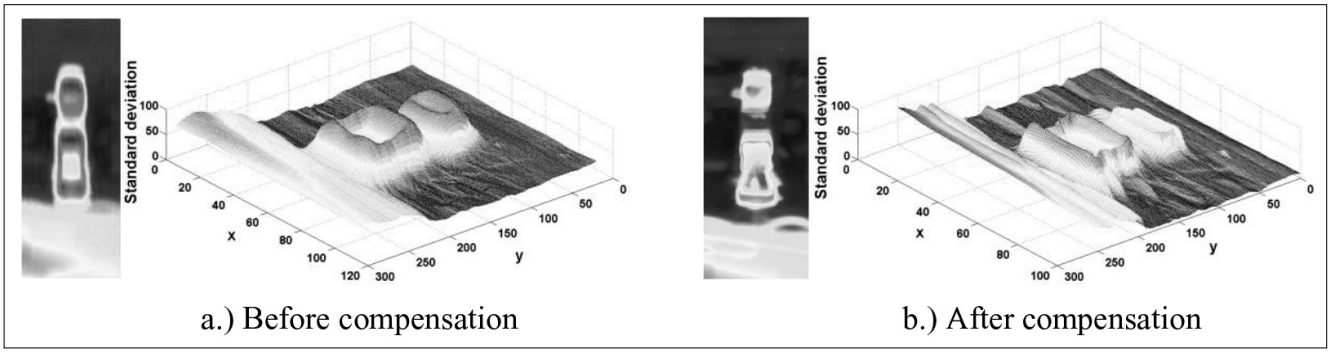

a.) Before compensation

b.) After compensation

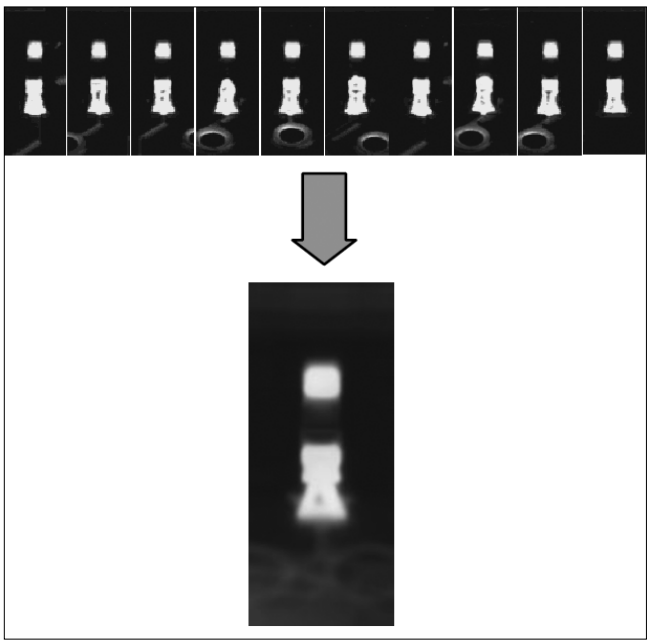

Figure 8. Example for a golden template (SOIC)

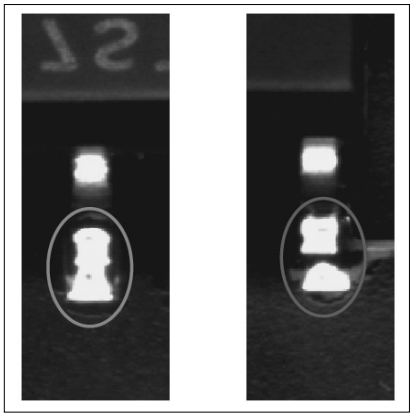

Figure 9. Illustration of small differences between good and bad images

$$gt(x,y) = \left(\mathrm{E}\left(\xi_{xy}\right)\right) \quad (2)$$

Certainly we have to estimate the expected values with the sample means therefore the resulted template image is the mean of all good images *(Fig. 8)*.

2.5.3 Split into subimages

As a next step, the algorithm determines the similarity between the images and the golden template. The differences between good and bad images can be occasionally very small and hard to detect (see *Fig. 9)*. Using general techniques by comparing whole images, these tiny (with size about 4x4 pixels) but very important dissimilarities get lost, implying that the class of error image cannot be found out.

Our new specialized technique splits the images into several small sub-images and the comparison method is executed on them separately and independently. The sub-images' size is much smaller than the original images' therefore the tiny errors contained only the good images become detectable on sub-images. The images are split with four different grids *(Fig. 10)* to avoid an important area being always divided between more sub-images. As our experiments show, the ideal size of a sub-image is about 8x8 pixels.

2.5.4 Calculation of difference profile

The split of an image results an image matrix which elements are the created sub-images. Next each sub-image will be compared with the corresponding area of the golden template generating the *difference profile* of the actual image.

In the simplest case, all pixels are taken into account with the same weight when computing the differences. But in a real situation, this assumption would distort the calculation. At some pixels of the image plane, the gray scale value of different images varies to a high degree. This means that several images differ very much from the golden template (from the expected value) at these regions. These high differences increase the values of the difference profile without reason, because the classification decision cannot be made by means of pixels where the gray scale value does not depend on the type of the image (namely it is bad or good).

This diversity of the gray scale values can be represented by standard deviation (or variance) of pixels' random variable. Large variance means that there are a lot of images in the actual image base which differ from the golden template at these regions to a high degree. *Fig. 11* illustrates two main places where the pixels' variance has huge value: at the sides of objects and at unimportant areas (i.e. not inspected by AOI macros). First instance occurs because the size and position differs to some degree despite earlier translation compensation therefore around the edges the pixels' value varies. At an unimportant part (second case) the AOI mac-

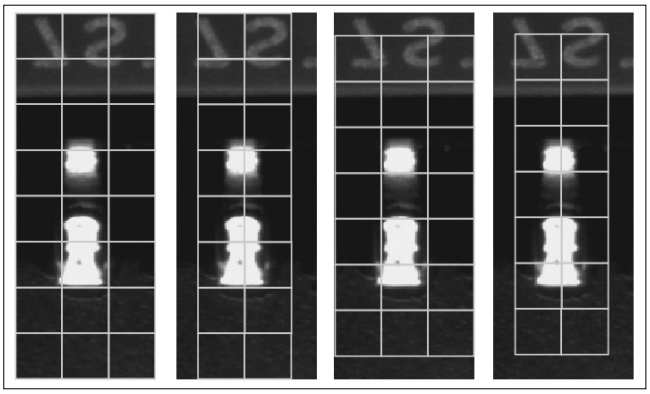

Figure 10. Grids to creates subimages

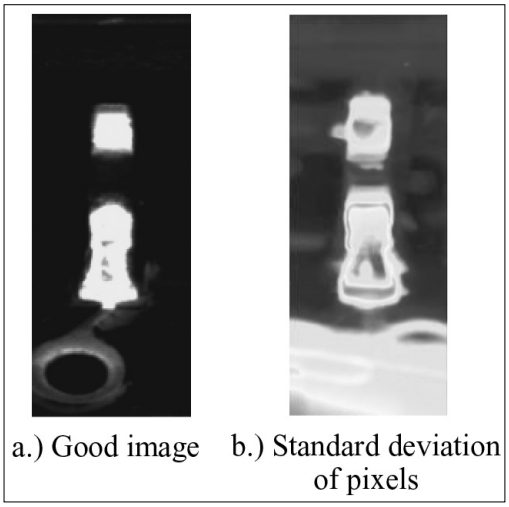

Figure 11. Illustration of standard deviation's role

ros do not inspect the images therefore at these areas also the good images can contain various pixel values causing high variance.

Our algorithm does not have any a-priori information about the images and about the AOI inspection macros. Hence it is not possible to remove these unnecessary regions before executing the comparing method. Therefore we used weighted distance metric to calculate the difference profile which considers also the variance of pixels.

Our method eliminates this problem by using weighted Euclidean distance where the weights are derived from the standard deviation of the actual sub-image. The greater the standard deviation of a pixel's random variables is, the smaller its significance. Therefore the weight function of *i*th and *j*th sub-image is the standard deviation matrix multiplied by minus 1 and scaled between 0 and 1:

$$W_{i,j}(x,y) = \frac{-\sigma_{i,j}(x,y) + \max\limits_{0\le k<N_{i,j};\,0\le l<M_{i,j}}\{\sigma_{i,j}(k,l)\}}{\max\limits_{0\le k<N_{i,j};\,0\le l<M_{i,j}}\{\sigma_{i,j}(k,l)\} - \min\limits_{0\le k<N_{i,j};\,0\le l<M_{i,j}}\{\sigma_{i,j}(k,l)\}} \quad (3)$$

where $\sigma_{i,j}(x,y)$ is the standard deviation function (matrix) of the sub-image, $N_{i,j}$ and $M_{i,j}$ are the dimensions of the sub-image. *Fig. 12* illustrates the result of this equation.

The scaling depends on the minimal and maximal level of the local (not the global) standard deviation field (namely only the actual sub-region of the golden template is considered). This means that the comparison is executed on each sub-image independently and the scaling takes the relative differences of a sub-region's variances into account.

We have tested several metrics like Euclidean distance, Manhattan distance, correlation etc. Our experiment shows that best choice is to use Euclidean distance.

As a result, the *i*th and *j*th element of the difference profile, namely the distances between the sub-image and golden template, can be calculated as follows:

$$D(i,j) = \sqrt{\sum_{k=0;\,l=0}^{N_{i,j}-1;\,M_{i,j}-1}\left(\left(gt_{i,j}(k,l) - subim_{i,j}(k,l)\right)^2 \cdot W_{i,j}(k,l)\right)} \quad (4)$$

where $gt_{i,j}(x,y)$ is the covered region of golden template, $subim_{i,j}(x,y)$ is the sub-image and $W_{i,j}(x,y)$ is the weight function determined earlier. *Fig. 13* illustrates two examples for the created difference profile.

2.5.5 Estimation of similarity degree

Difference profile contains the error values of image's sub-regions. We have deduced the similarity degree from analysing this error field.

We have considered several metrics of difference profiles, like maximal and minimal values, average value, variance (standard deviation) etc. Our experiments show that it is hard to distinguish the sets of good and bad images by means of only one feature.

Fig. 14 illustrates that neither maximal error value, nor the standard deviation of the difference profile, as the two most relevant metrics, can separate bad images from good images by themselves. But the simultaneous usage of both techniques yields a 2-dimensional metric which combines their advantages and creates a simi-

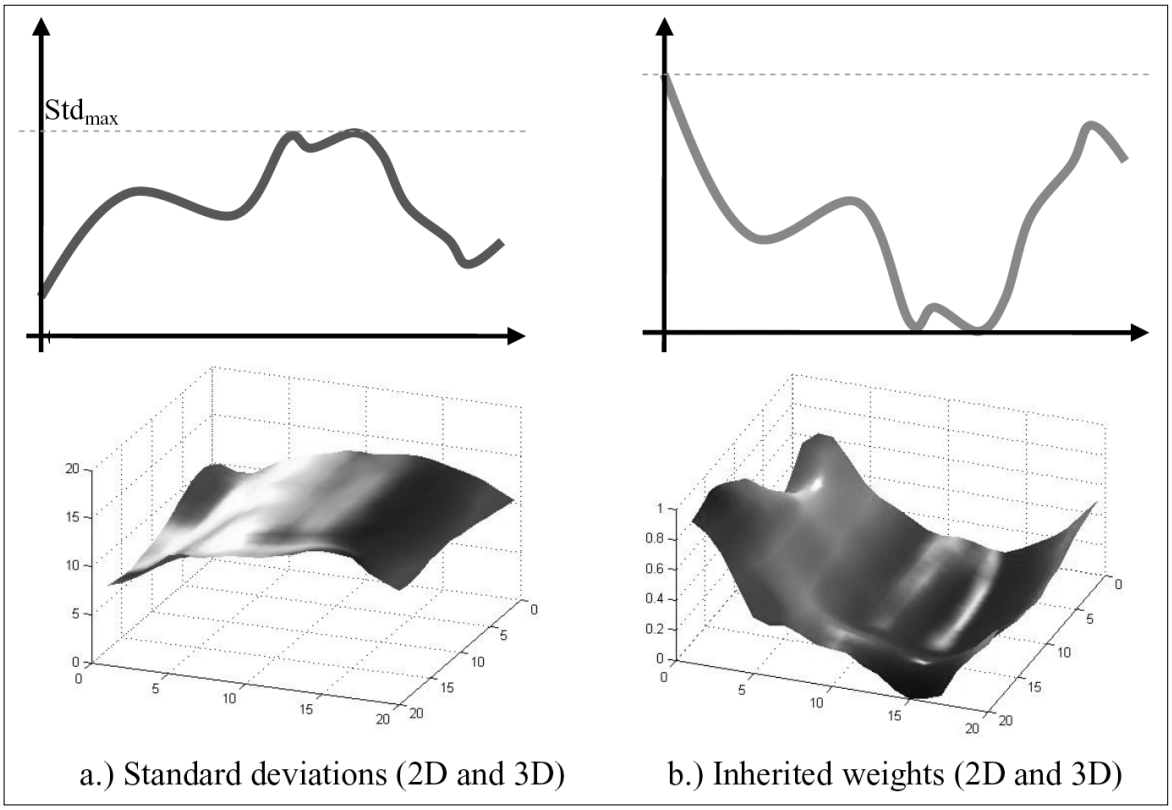

Figure 12. Examples for weighting functions

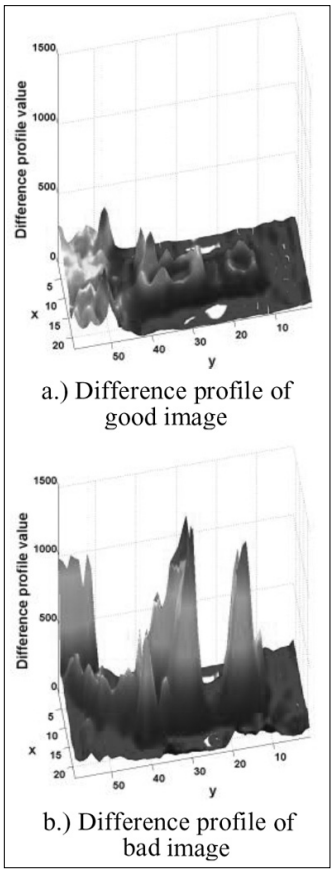

Figure 13.
Examples for difference profile (SOIC)

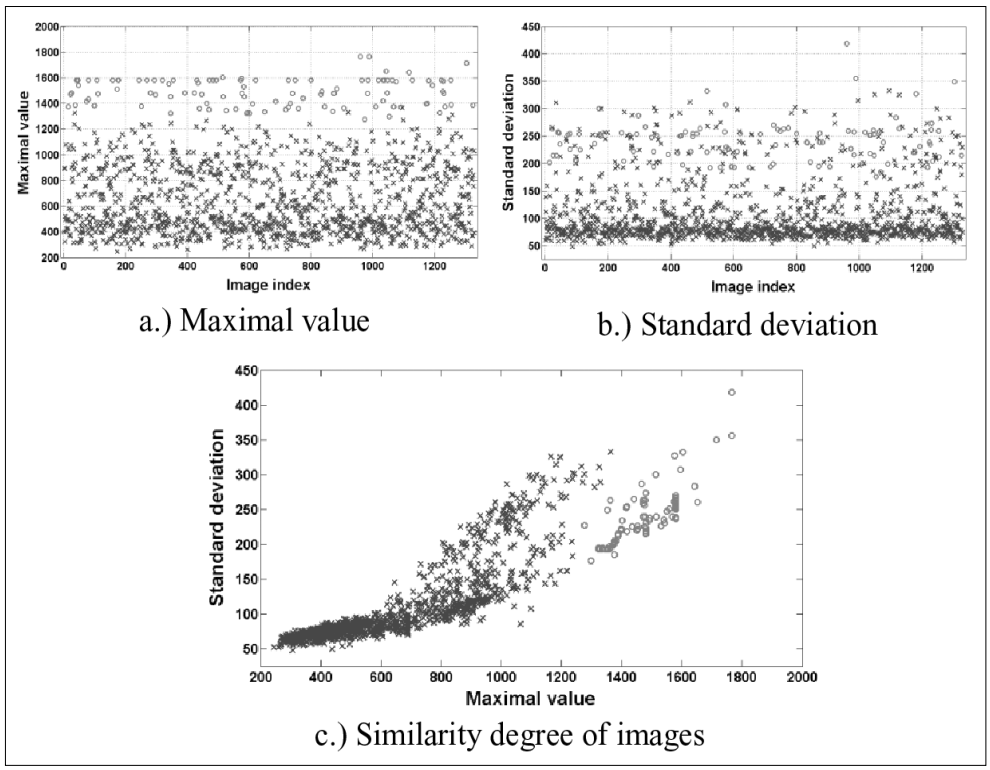

Figure 14. Examples for similarity degrees (SOIC)

larity degree field where the two image groups can be relatively well separated (Fig. 14). This field gives an excellent basis for the next classification method.

2.6 Summary

The flowchart in *Fig. 15* summarizes the working process of our similarity degree calculation. First the positions are equalized and the golden template is calculated which is the expected value of good images. Next the images are split into small sub-images, otherwise the small but very important errors on images would get lost by comparing the whole images. At the third step, we calculate the difference profile which is the weighted Euclidean distance between the sub-regions of the images and the golden template. The weights are inherited from the standard deviation of the local region. The similarity degree of an image is a 2-dimensional vector derived from the maximal difference value and the standard deviation of the difference profile.

3. Experiments

In previous section, we explained the calculation process of similarity degrees. After computation, a 2-dimensional similarity degree field is generated where all images is projected in. Analysing this vector field, important AOI problem can be solved without serious additional work. In this paper, we will present two important areas where we used our method with significant success (see *Fig. 16)*.

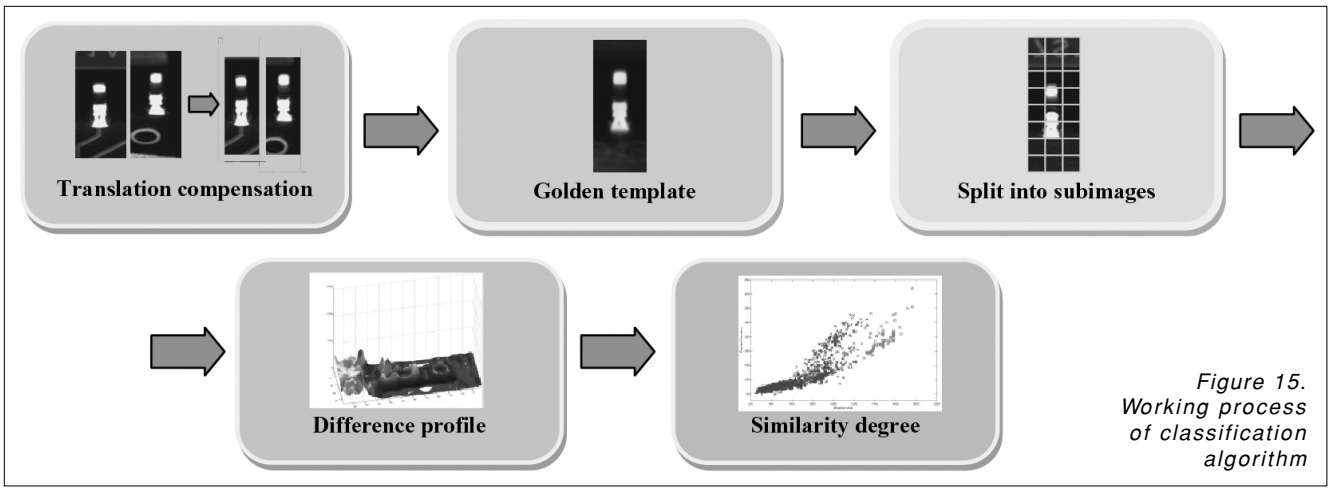

Figure 15. Working process of classification algorithm

3.1 Decision support in re-inspection phase

In Section 2.1, we introduced that, after the AOI inspected the PCB, a human operator checks again the determined errors. This is because of small modification in manufacturing process generates false alarms (namely the AOI device classified a good component as faulty) which are revised by human experts. This human-machine cooperation would create a great inspection system because the devices are very fast and accurate, while the humans are not. But unfortunately, the need of human factor decreases the reliability and productivity of the manufacturing and the inspection process. Therefore it is aimed to develop techniques to assist the human operators' work in re-inspection process. Our purpose was to create a re-inspection system which compares the error images (on which a bad component was found by AOI device) with a reference database, and by means of the comparing information takes a proposal for the human operator about the appropriate class of the image (see Fig. 16).

The technique of "learning and recognizing" in AOI systems appeared already in earlier publications. In general, the researchers use neural networks in inspection systems [1,2,5,18]. In spite of this, we would like to avoid the utilization of artificial neural networks in automated optical inspection. Although the neural networks make exact, repeatable calculations and in general do not contain any stochastic steps, they are "black boxes" from the point of view of the engineers who are responsible for quality inspection in the whole factory, because it is hard or impossible to convert the connection forces (weights) between neurons in a trained neural network to exact physical meaning of optical inspection and measurement.

The training of neural networks raises also an interesting question. Our task is to pre-classify the error images in two groups: good images (false-calls) and bad images (real errors). There are several samples in the first group, but much less real images exist. Until the false-call images are relative similar to each other, the real errors have numerous appearances. Therefore in field of the training process and working quality, more difficulties and challenges occur.

These facts motivated us to advance in another development direction. The similarity degree analysis is a very good basis of a decision support system. The algorithm is based on the fact that false-call images cannot satisfy the serious requirements of AOI macros, but they are very similar to normal (good) and to other false-call images. Therefore if an error image seems like stored good images, it is probably also a good image; if the image is dissimilar, the algorithm suggests that it shows a real error. By means of the similarity measurement field it is possible to decide about a new error image, that it contains a good or a bad component.

At calibration, the golden template and the reference images' similarity degrees are calculated. At re-inspection process, the algorithm determines the similarity degree of the actual error image (by means of earlier calculated golden template) and places the value on the 2-dimensional similarity degree field. The proposed class of error image is determined by three different factors: class of nearest image, class of image-group belong to the smaller average distance, clustering result (details are explained in Section 3.2). The classification method calculates all of these metrics and the voting result determines the final class of error image: if already one metric signs that the error image contains real error, the image is classified as bad.

We will present the most important results in Section 3.2. The decision support system based on our novel similarity measurement method can separate the good and bad pictures with very small error rate, independent from the type of images. The method does not use image base specific settings (except the type of reference point at translation compensation), and it works without any modification on several AOI image bases equally well.

Figure 16. Model of AOI systems completing with our novel methods

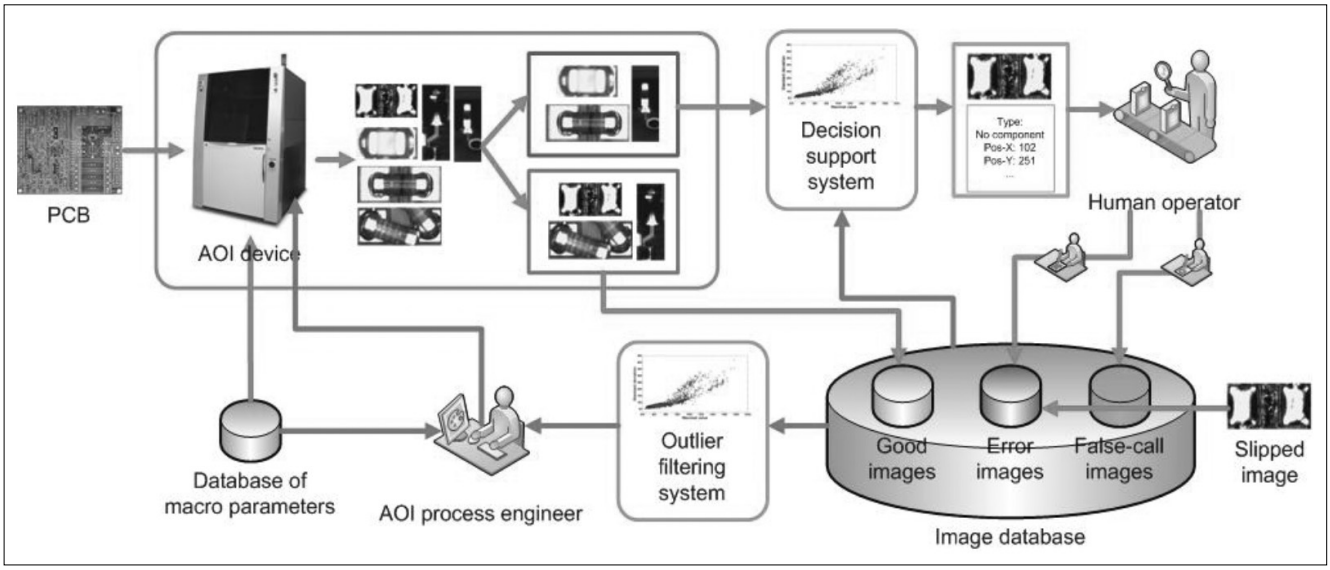

3.2 Outlier filtering in AOI image databases

The presented cooperation between machines and humans implies special difficulties in the topic of optical inspection. An interesting and important challenge is the faulty content of image databases storing previously created inspection images, namely during image collection – mainly caused by human factor – some falsely classified images can be put in the image database. This means that image bases, which normally include pictures showing only good components, contain also images with bad components. This occurrence makes, for example, the optimization process impossible because it is always assumed that the training image bases are homogenous. It causes less accurate AOI systems, higher optimization cost and prevent the development of fully-autonomous AOI devices.

The image database filtering algorithm is typical outlier detection task [7,8,10]. There are several methods published in the topic of image processing outlier detection [13,15,19-21,23]. Most frequently, it is used in medical imaging and analysis of satellite images, but it has high significance in other image processing areas as well. Compared to these methods, the environment of our algorithm has very special requirements. First of all, the usage of training samples is entirely intolerable because creation of training samples and keeping them in good condition are hard and very time-consuming processes in case of manufacturing. Another very important condition is that the whole image – not only some features – need to be considered by identifying the outliers, because the AOI images contain very important information on the full image plane (except at narrow region of images' side).

The last important difference between this algorithm and earlier published methods is that our technique does not know what kind of outliers can occur on falsely classified images. This means, that our algorithm gets an image database as input, without any information about features why an image is an outlier. Our method "finds out" these differences in case of each AOI image set separately, apart from the component what the images contain. This is a novel aspect in the area of outlier detection in image processing systems.

The similarity degree field gives a very essential solution for this application. The similarity degree belong to all the images in the database under filtering will be calculated and by analysing the produced similarity vector field, the outliers can be detected.

It was introduced in Section 2.5.2 that the golden template is really the mean of all good images. Certainly, this creation method is impossible because the usage of training samples is excluded. Therefore by calculating the mean image, all the images are considered as well. The number of outlier images is much less than the number of well-classified images therefore the mean image cannot be damaged much by the outlier images. *Fig. 17* shows a mean image created with (*a*) and without (*b*) outlier images. It is apparent that the differences between the images are negligible (*c*).

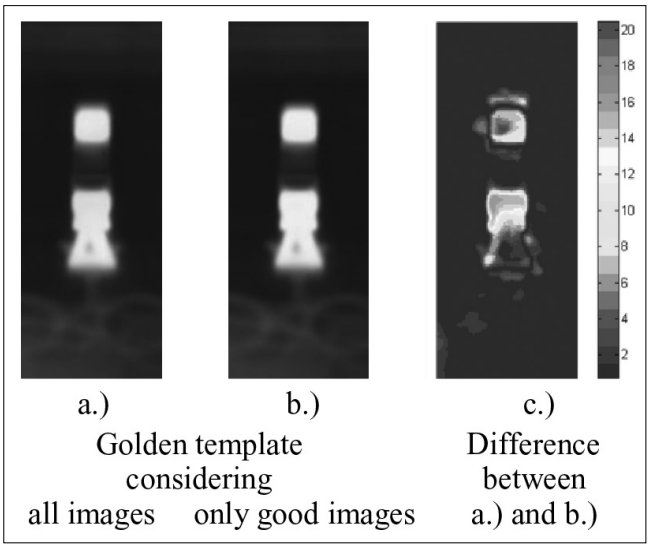

Figure 17. Effect of outlier images in golden template

After calculating the similarity degree (by means of the special golden template), it is necessary to separate the whole set into two subsets (well-classified and outlier images). We applied the well-known k-means algorithm [9,16] to cluster the similarity degree field in two groups. In our method, it is created 5 clusters ($k = 5$), because of special locations of well-classified and outlier points. Because the clustering depends on the starting parameters of the k-means method, the clustering is executed more times with different starting arguments to find all possible outliers.

In *Fig. 18*, a clustering result is shown (SOIC). The graph illustrates that all of the outlier image were found, and only 7 well-classified images are classified badly, which is smaller than 0.005% error rate. (The detailed results are explained in next section.)

3.3 Results

We tested both algorithms on several image databases which were created at an industrial production line. Each image database contains good (well-classified) and bad (outlier) images. *Table 1* presents the image databases used.

Figure 18. Result of clustering algorithm in case of 5 clusters

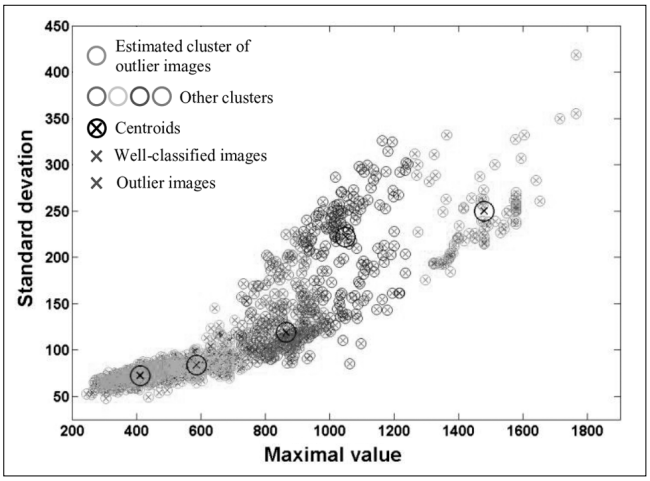

We used the same image databases in both algorithms. In case of decision support system, half of images were the training samples, the other half of them were the testing elements. The quality factor was that how many testing image are classified well. In outlier filtering method, all the images in a database were created the original (unfiltered) image set and the purpose was to filter only the bad images. It is important to note that on every image base the same algorithms (with the same parameters) were executed. There were no special settings or adjustments for single image sets.

Table 2 shows the result of 7 image databases. First it is important to note that the qualities of two algorithms are very similar: at same databases both methods have quite the same results. This is because both techniques are built on the same basis (on analysis of similarity degree field) therefore this identity is not surprising.

The results in the table show that both methods were able to execute their tasks with very small error rate: the general hit rate is greater than 98%. At decision support system, in five cases all real error images were found, in the remaining two image sets only some special error could not be identified well. In case of outlier filtering method, all outliers were found in five databases, in the other two image bases the classification rates were above 96%.

The best results were noticeable in both cases in image database of C0805, C1210, SMCTAB and SOIC. The algorithms could separate the good and bad images almost perfectly. The result speaks for itself, it is not necessary to analyse this conclusion further.

At the MELF and SMCTAC image bases, "only" 94-97% of real errors or outliers were detected. *Fig. 19* shows that very small regions contain the differences, and at these areas, the pixel's standard deviation has a relatively high value. In spite of these difficulties, our method assigns relatively low similarity degree to these pictures, but at those points in similarity degree plane, the density of good images is higher and the classification algorithm classifies these pictures in the false group.

In case of R0805, the number of badly clustered good images is relatively high (~10%). The reason is that in this image base, the good images are very different from each other (see *Fig. 20)*. Therefore it is quite hard to determine the regions where the good and bad images differ which caused the high rate of false positive errors. Here the question about the usability of the algorithm in industrial production can occur, but it is important to note two facts. First, all real error images or outliers were detected, which more important task in case of manufacturing. Second, looking at Fig. 20, we can see the high heterogeneity of the good images which is a very serious challenge for all classification methods (an also for human experts). The 10% false positive rate in this adverse environment is an acceptable result, also in industrial production.

An important feature of this algorithm is that the classification decision is executed without using any threshold parameters, but it uses a standard clustering technique. Moreover, the method does not use image base specific settings (except the type of reference point at translation compensation), but it calculates the inner

C0805	Capacitor with standard size 0805	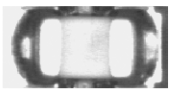	Number of images: **1342** Good: **1221** (90.98%) Bad: **121** (9.02%)
C1210	Capacitor with standard size 1210		Number of images: **1405** Good: **1306** (92.95%) Bad: **99** (7.05%)
MELF	Metal electrode leadless face diode	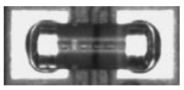	Number of images: **1576** Good: **1451** (92.07%) Bad: **125** (7.93%)
R0805	Resistor with standard size 0805		Number of images: **1086** Good: **1011** (93.09%) Bad: **75** (6.91%)
SMCTAB	Surface mount capacitor with size „B"		Number of images: **1174** Good: **1119** (95.32%) Bad: **55** (4.68%)
SMCTAC	Surface mount capacitor with size „C"		Number of images: **1384** Good: **1274** (92.05%) Bad: **110** (7.95%)
SOIC	Small-outline integrated circuit		Number of images: **1329** Good: **1221** (91.87%) Bad: **108** (8.13%)

Table 1. Image databases for testing

Image type	Decision support system		Outlier filtering method
	Good image	Bad image	
C0805	Well classified: **609** (99.84%) Badly classified: **1** (0.16%)	Well classified: **60** (100%) Badly classified: **0** (0%)	Found outliers: **121** (100%) Well-classified images in good cluster: **1218** (99.75%) Well-classified images in outlier cluster: **3** (0.25%)
C1210	Well classified: **649** (99.39%) Badly classified: **4** (0.61%)	Well classified: **49** (100%) Badly classified: **0** (0%)	Found outliers: **99** (100%) Well-classified images in good cluster: **1302** (99.69%) Well-classified images in outlier cluster: **4** (0.31%)
MELF	Well classified: **715** (98.62%) Badly classified: **10** (1.38%)	Well classified: **60** (96.77%) Badly classified: **2** (3.23%)	Found outliers: **121** (96.80%) Well-classified images in good cluster: **1441** (99.31%) Well-classified images in outlier cluster: **10** (0.69%)
R0805	Well classified: **456** (90.30%) Badly classified: **49** (9.70%)	Well classified: **37** (100%) Badly classified: **0** (0%)	Found outliers: **75** (100%) Well-classified images in good cluster: **914** (90.40%) Well-classified images in outlier cluster: **97** (9.60%)
SMCTAB	Well classified: **557** (99.64%) Badly classified: **2** (0.36%)	Well classified: **26** (100%) Badly classified: **0** (0%)	Found outliers: **55** (100%) Well-classified images in good cluster: **1097** (98.03%) Well-classified images in outlier cluster: **22** (1.97%)
SMCTAC	Well classified: **633** (99.37%) Badly classified: **4** (0.63%)	Well classified: **52** (94.55%) Badly classified: **3** (5.45%)	Found outliers: **106** (96.36%) Well-classified images in good cluster: **1263** (99.14%) Well-classified images in outlier cluster: **11** (0.86%)
SOIC	Well classified: **609** (99.84%) Badly classified: **1** (0.16%)	Well classified: **54** (100%) Badly classified: **0** (0%)	Found outliers: **108** (100%) Well-classified images in good cluster: **1214** (99.43%) Well-classified images in outlier cluster: **7** (0.57%)

Table 2. Testing results

parameters automatically only by means of actual image database without any external information. Therefore it is hard or impossible to modify the ratio of false positive and false negative errors only by means parameters, so general experiment methods, like ROC curve analysis, were avoided.

One of the most important requirements of the research was to find all real errors or outliers (no or very small false negative error), during the false positive rate stays below a quite low limit. The results mentioned above illustrate, that our general methods based on similarity degree can separate the good and bad pictures with very small error rates, independently from the type of images.

4. Conclusions

This paper presented a novel image similarity measurement method for AOI image databases. The algorithm calculates first a golden template image which represents the average image of good components. Next the image under inspection is compared with this golden template on the level of sub-regions, creating the difference profile. The analysis of this error field (maximum value and standard deviation) results the 2-dimensional similarity degree which symbolize how close the actual image is to the golden template. This means, that the developed similarity degree is a relative measurement value.

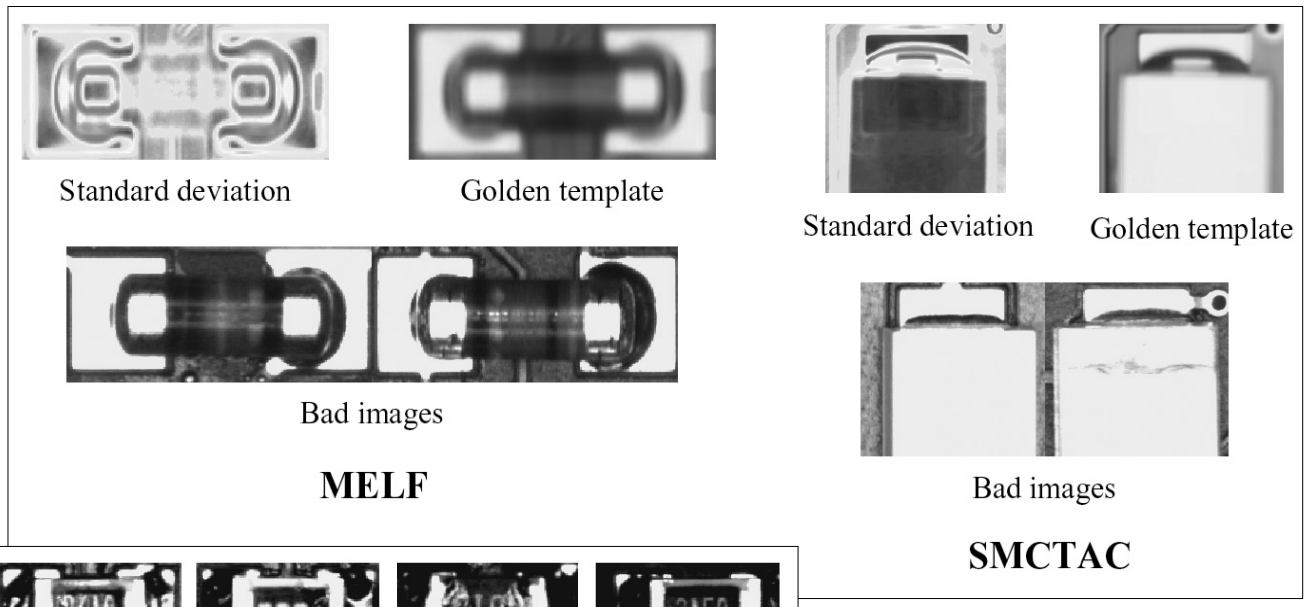

Figure 19.
Illustration of bad classification result

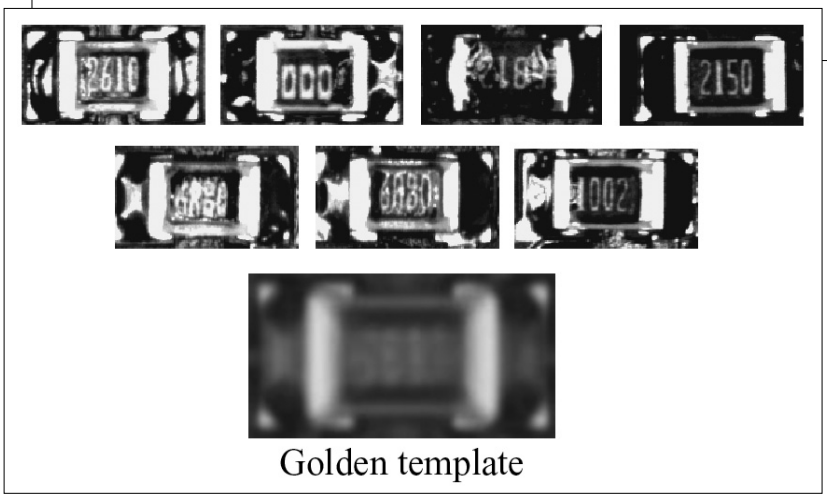

Figure 20.
False-call images in R0805 image base

By means of this measurement method (by analysing the similarity degree vector field), important AOI problem can be solved without serious additional work. This article presented two interesting area: decision support system for human operators at re-inspection process; outlier detection method for filtering the AOI image databases. In the first case, the algorithm uses training images about good and bad components, and calculates their similarity degree vectors.

At re-inspection process, the algorithm determines the similarity degree of the actual error image and determines the appropriate class by means of three different factors (nearest image, smaller average distance, clustering result). The outlier filtering algorithms estimates the golden template as the mean image of all (bad and good) pictures in the database, and by means k-means clustering separates the well-classified and outlier images.

We tested our algorithm on seven different image bases which contain different types of components, like SMT capacitors, resistors, or pins. The experiments show excellent results: in five cases, all real errors or outliers were classified perfectly, in the remaining two image bases the classification rates were 94-97%. The false classification of good images was below 2% in average. This means that our novel decision support and filtering methods based on novel similarity degree calculation are useful also in industrial applications at this stage of our research already. We would like to emphasize again, that our algorithms do not apply outer parameters, they calculate all the stages only by means of actual image database, and they work without any modification on several different types of AOI image bases well.

Authors

TIBOR TAKÁCS received his Master degree in Computer Science from Budapest University of Technology and Economics in 2007. He is currently working as a Ph.D. candidate at the Department of Control Engineering and Information Technology. His research interest focuses on optimization problems, novel image processing techniques and intelligent solutions in automated optical inspection systems.

LÁSZLÓ VAJTA received his Ph.D. degree in Electrical Engineering in 2005 from Budapest University of Technology and Economics, and is currently working as an associate professor at the Department of Control Engineering and Information Technology. His main research activities focus on image processing system and on the area of machine vision solutions.

References

[1] Acciani, G., Bruneti, G., Fornarelli, G., A Multiple Neural Network System to Classify Solder Joints on Integrated Circuits, Int. Journal of Computational Intelligence Research, ISSN 0973-1873, Vol. 2, No. 4, pp.337–348, 2006.

[2] Acciani, G., Bruneti, G., Fornarelli, G., Application of Neural Networks in Optical Inspection and Classification of Solder Joints in Surface Mount Technology, IEEE Transactions on Industrial Informatics, Vol. 2., No. 3, pp.200–209, 2006.

[3] Balakrishnan, N., Handbook of the logistic distribution, Marcel Dekker, ISBN 0824785878, 1991.

[4] Barnett, V., Lewis, T., Outliers in statistical data (3rd ed.). John Wiley&Sons, ISBN 0471930946, 1994.

[5] Belbachir, A.N., Lera, M., Fanni, A., Montisci, A., An automatic optical inspection system for the diagnosis of printed circuits based on neural networks, Industry Applications Conference 2005, 48th IAS Annual Meeting, Conf. Record of the 2005, ISBN 0-7803-9208-6, pp.680–684 (Vol. 1), 2005.

[6] Gonzalez, R.C., Woods, R.E., Digital Image Processing (3rd ed.), Prentice Hall, ISBN 9780131687288, 2008.

[7] Grinstead, C.M., Snell, J.L., Introduction to Probability, ISBN-10 0821807498, ISBN-13 978-0821807491, 1997.

[8] Grubbs, F. E., Procedures for Detecting Outlying Observations in Samples. Technometrics (Vol. 11), pp.1–21, 1969.

[9] Hartigan, J.A., Clustering Algorithms. John Wiley&Sons, 1975.

[10] Hodge, V., Austin, J., A Survey of Outlier Detection Methodologies. Artificial Intelligence Review, Springer, Vol. 22, No. 2, pp.85–126, 2004.

[11] Hogg, R.V., Craig, A., Introduction to Mathematical Statistics (5th ed.), Prentice Hall, ISBN-10 0023557222, ISBN-13 9780023557224, 1994.

[12] Kong, F., Wang, Y., Reconstruction of Solder Joint Surface Based on Shape from Shading, 3rd Int. Conf. on Natural Computation (ICNC 2007), ISBN 9780769528755, pp.58–62, 2007.

[13] Lee, C.S., Elgammal, A., Dynamic shape outlier detection for human locomotion, Computer Vision and Image Understanding, Vol. 113, pp.332–344, 2009.

[14] Lipson, P. R., AOI Systems Simulate Human Brain. Test & Measurement World, pp.35–42, 2007.

[15] Lu, C. T., Kou, Y., Zhao, J., Chen L., Detecting and tracking regional outliers in meteorological data. Information Sciences, No. 177, pp.1609–1632, 2007.

[16] MacKay, D., Information Theory, Inference and Learning Algorithms, Cambridge University Press, ISBN-10 0521642981, ISBN-13 9780521642989, 2003.

[17] Mar, N.S.S., Fookes, C., Yarlagadda, P.K.D.V., Design of automatic vision-based inspection system for solder joint segmentation, Journal of Achievements in Materials and Manufacturing Engineering, Vol. 34. Issue 2, pp.145–151, 2009.

[18] Ong, T.Y., Samad, Z., Ratnam, M.M., Solder Joint Inspection with Multi-angle Imaging and Artificial Neural Network, The International Journal of Advanced Manufacturing Technology, Springer London, ISSN 0268-3768 (Print), 1433-3015 (Online), Vol. 38, No. 5-6, pp.455–462, 2007.

[19] Petrakis, E.G.M., Faloutsos, C., Similarity Searching in Medical Image Databases. IEEE Trans. on Knowledge and Data Engineering, Vol. 9, No. 3, pp.435–447, 1997.

[20] Prastawa, M., Bullitt, E., Ho, S., Gerig G., A brain tumor segmentation framework based on outlier detection. Medical Image Analysis, pp.275–283, 2004.

[21] Vellidoa, A., Lisboab, P.J.G., Handling outliers in brain tumour MRS data analysis through robust topographic mapping, Computers in Biology and Medicine, Vol. 36, Issue 10, pp.1049–1063, 2006.

[22] Wang, D.Z., Wu, C.H., Ip, A., Chan, C.Y., Wang, D.W., Fast Multi-template Matching Using a Particle Swarm Optimization Algorithm for PCB Inspection, Lecture Notes in Comp., No. 4974, pp.365–370, 2008.

[23] Zhan, Y., Advanced image analysis methods for the diagnosis of prostate cancer. (PhD dissertation), ISBN/ISSN 978 05493 14134, 2008.